NATIONAL ADVISORY COMMITTEE FOR AERONAUTICS

TECHNICAL NOTE 2897

EVALUATION OF GUST RESPONSE CHARACTERISTICS OF SOME EXISTING AIRCRAFT WITH WING BENDING FLEXIBILITY INCLUDED

By Eldon E. Kordes and John C. Houbolt

Langley Aeronautical Laboratory
Langley Field, Va.

Washington
February 1953

NATIONAL ADVISORY COMMITTEE FOR AERONAUTICS

TECHNICAL NOTE 2897

EVALUATION OF GUST RESPONSE CHARACTERISTICS OF SOME EXISTING AIRCRAFT WITH WING BENDING FLEXIBILITY INCLUDED

By Eldon E. Kordes and John C. Houbolt

SUMMARY

Calculation studies made by means of the analysis presented in NACA TN 2763 to evaluate the influence that wing bending flexibility has on the structural response to gusts are reported for three twin-engine transports and one four-engine bomber. The manner in which dynamic response factors for acceleration and bending moment vary with different assumed airplane operational factors is shown. Factors investigated include gust-gradient distance, gust shape, spanwise mass distribution, forward velocity, altitude, and compressibility and aspect-ratio corrections. An evaluation of the gust response characteristics for all four airplanes is given; it is found that three of the airplanes have rather appreciable elastic-body dynamic-overshoot effects but one does not. A rule of thumb is suggested for judging when airplanes may be considered rigid for discrete gust encounter. A limited correlation of some of the calculated results with flight data is also presented.

INTRODUCTION

In many newer aircraft, the speed has become sufficiently high and/or the frequencies of the structural modes of vibration (particularly fundamental wing bending) sufficiently low so that the treatment of the aircraft as a rigid body in the design for gust loads can no longer be considered adequate. The extent to which elastic-body dynamic effects should be taken into account in design or are present when the airplane is used as an instrument for measuring gust intensity is therefore of great interest.

As a part of the general study being made to investigate the role that wing bending flexibility plays in the structural response of an airplane penetrating a gust, several existing aircraft have been considered and calculations of the response (accelerations and bending moments) to gust encounter of these airplanes have been made for a

variety of assumed flight conditions. The purpose of this report is to present the results of these calculations, since many of the trends found are believed to be applicable to many other aircraft.

Specifically, four airplanes have been considered; three are twin-engine transports and one, a four-engine bomber. The method of analysis used to treat these airplanes is that given in reference 1, which considers the airplane to have two degrees of freedom, vertical motion as a rigid body and wing bending.

The calculations were made for the condition of a single gust encounter and were divided into two phases. In the first phase the aim was to show how the response for wing bending moment is affected by variations in certain assumed airplane operating conditions or by different choices in some of the aerodynamic factors involved. Two of the transports were used in this phase. In the second phase the aim was to study how wing bending flexibility might influence gust measurements if such measurements are made with these aircraft. Flight tests made in clear rough air with one of the transports and the bomber have indicated that the measured center-line accelerations (the values commonly used in estimating the gust intensities) can be from 20 to 28 percent greater on the average than the true or rigid-body component of acceleration (see refs. 2 and 3). It was considered of interest to see what discrete-gust calculations reveal in this respect. Results for bending moment and accelerations are first given to show the degree of flexibility of each of the four airplanes. Then a limited correlation of the acceleration results for the two airplanes that were flight-tested is made with the flight data.

SYMBOLS

A	aspect ratio of wing
a	lift-curve slope
$b/2$	semispan of wing
c_o	wing reference chord
g	acceleration due to gravity
H	gust-gradient distance (distance to point of maximum gust velocity), chords
K_{root}	nondimensional bending-moment factor $\left(M_{root} = \frac{a}{2} \rho V U M c_o K_{root}\right)$

M	Mach number
M_{root}	incremental bending moment at wing root station
M_{c_0}	first moment of wing area about wing root station
Δ_n	incremental number of g acceleration
r_n	nondimensional area parameter (see ref. 1)
S	wing area
T_G/T_1	period ratio, time required to penetrate gust to point of maximum gust velocity divided by one-fourth the natural period of fundamental wing bending mode, $\frac{4}{\pi}\lambda H$
U	maximum vertical velocity of gust
V	forward velocity of flight
W	total weight of airplane
y	distance along wing measured from airplane center line
γ_a	response factor for accelerations, maximum acceleration at center line divided by maximum acceleration at nodal points of fundamental mode
γ_M	response factor for bending moments, maximum incremental bending moment for flexible wing divided by maximum incremental bending moment obtained when wing is considered rigid
λ	reduced-frequency parameter, $\frac{c_0\omega_1}{2V}$
μ_n	mass parameter (see ref. 1)
η_n	bending-moment parameter (see ref. 1)
ρ	mass density of air
$1 - \Phi$	function which denotes growth of lift on an airfoil following a sudden change in angle of attack (Wagner function)

ψ function which denotes growth of lift on a rigid wing entering a sharp-edge gust (Küssner function)

ω_1 natural circular frequency of fundamental mode

Subscript:

max maximum

DESCRIPTION OF AIRPLANES STUDIED

The three transports are herein designated as airplanes A, B, and C, and the bomber, as airplane D. Airplane B is a revised model of airplane A; the primary changes are in the wing mass distribution and wing stiffness, the wing plan form being the same. The spanwise variations of weight, chord, and bending moment of inertia for each of these airplanes are given in figures 1 to 3. Table 1 lists the physical constants and basic parameters that are required to treat these airplanes by the method given in reference 1. The values of the parameters μ_0, μ_1, λ, η_0, and η_1 in this table are the values obtained when a lift-curve slope of 2π and a midspan reference chord are used. The table also indicates the approximate disposition of movable load (fuselage load and fuel) that was considered in the calculations.

EFFECT OF OPERATIONAL CONDITIONS ON BENDING MOMENT

In order to evaluate how the structural response of an airplane penetrating a gust is influenced by wing bending flexibility, one approach is to apply the method given in reference 1 and to investigate how the calculated response is affected by individual variations in the basic parameters μ_0, μ_1, λ, η_0, η_1, and H that are established in that reference. This approach, however, has the drawback that, for the majority of these parameters, it is difficult to attach a clear physical interpretation to what occurs when individual variations are made. A perhaps more instructive approach from the point of view of retaining a physical insight is to consider some existing aircraft and to examine how the calculated structural response (such as bending moment) is affected by assumed changes in operating conditions or by changes in the aerodynamic factors that are present in the equations for response. Such changes may alter one or several of the aforementioned basic parameters; for example, a change in the velocity alters the value of λ only, but a change in either the altitude or the slope

of the lift curve will cause a simultaneous change in each of the four parameters μ_0, μ_1, η_0, and η_1. The latter approach has been adopted herein and the bending moment has been chosen as the index of the structural response.

Specifically, the factors considered have been limited to the following:

(a) Gust-gradient distance

(b) Gust shape

(c) Spanwise mass distribution

(d) Forward velocity

(e) Altitude

(f) Compressibility and aspect-ratio corrections

The influence of these factors on the bending moment that is developed during a single gust encounter has been investigated by means of airplanes A and B. Only gusts uniform in the spanwise direction were considered and, for all but item (f), calculations were made by using the theoretical lift-curve-slope value 2π and the indicial lift functions $1 - \Phi$ and ψ for two-dimensional incompressible flow. In presenting the results to follow, a period ratio $\frac{T_G}{T_1} = \frac{4}{\pi}\lambda H$ has been introduced, where T_G is the time required for the airplane to penetrate the gust to the point of maximum gust velocity and T_1 is one-fourth the natural period of the fundamental wing bending mode. This ratio has been included because a similar period ratio, that is, the ratio of the period of the applied force to the natural period of vibration of the structure, has been found to be significant in response calculations of elastic structures under dynamic loading and it was considered of interest to see whether such a ratio has a similar significance for structures under gust loading.

Effect of gust-gradient distance.- In the investigation of the effect of gust-gradient distance, airplane A (see table 1) is assumed to fly with a velocity of 255 mph through sine gusts of various gradient distances. The response obtained is shown in figure 4; the lower curves give the variation of the maximum root bending-moment factor $(K_{root})_{max}$ with gust-gradient distance H and the period ratio T_G/T_1. This factor may be used to calculate the maximum net incremental bending moment (combined aerodynamic and inertial) developed at the root from the expression (see ref. 1)

$$(M_{root})_{max} = \frac{a}{2}\rho V U M c_0 (K_{root})_{max} \qquad (1)$$

Values of $(K_{root})_{max}$ are shown for the wing considered flexible as well as for the wing considered rigid. The difference between these two curves may be considered as a dynamic-overshoot effect; the ratio of the ordinates of the two curves (flexible to rigid) leads to the curve for response factor γ_M shown in the upper part of the figure. (Although not shown for values of H less than 1, this curve is found to pass through the origin.) The results indicate that for the airplane considered there may be a dynamic overshoot up to 25 percent for intermediate gust-gradient distance but that the airplane acts essentially as a rigid body for values of H greater than about 9 chords or T_G/T_1 greater than about 4.5.

Effect of gust shape.- From time to time the question has been raised as to the influence that gust shape has on airplane response. In order to obtain a measure of this effect, airplane A was again used and was assumed to fly with a velocity of 255 mph through single gusts having three different shapes, a sine shape, a sine^2 shape, and a triangular shape. The bending-moment response factor obtained for these different gust shapes, as it varies with the gradient distance and the period ratio, is shown in figure 5. The results on the whole are not significantly different, although it may be seen that the response curve for the sine^2 gust is displaced somewhat to the right of the curves for the sine and triangular gusts. This shift to the right is undoubtedly due to the rather slow rate of change in gust velocity during the initial portion of the sine^2 gust, and suggests, as might be expected, that a sine^2 gust of a given length is roughly equivalent to a sine (or triangular) gust of a slightly shorter length. Although these results are for one airplane and one loading condition, similar results are expected for other airplanes and loading conditions.

Since gust shapes do not cause major changes in the results, the sine gust has been arbitrarily chosen for subsequent calculations in this phase.

Effect of spanwise mass distribution.- In examining the effect of spanwise mass distribution, airplane B was used since the fuel load carried by airplane B is greater and extends over a greater portion of the semispan than the fuel load carried by airplane A. For this study the gross weight was held essentially constant and the following three loading conditions were considered: the previous loading condition of one-half fuselage load and one-half fuel load, the condition of zero fuselage load and full fuel load, and the condition of full fuselage load and zero fuel load. The results for a velocity of 255 mph are shown in figure 6, where the three loading conditions are indicated by schematic sketches. Figure 6(a) shows that the response factor becomes

greater and remains large over an increased range of gradient distance as the disposable load is moved outboard on the wing. These results thus indicate that there is an appreciable change with loading condition of the value of H at which the response curves become essentially unity. If presented in terms of T_G/T_1 instead of H, however, the results condense much better. The response curves now all peak together at a value of T_G/T_1 of approximately 1.5 and, further, they all become essentially unity (within a few percent) at a value of T_G/T_1 of roughly 5. The latter fact suggests that T_G/T_1 might make a good index for judging whether wing flexibility has to be taken into account. Specifically, the rule of thumb suggested is that as long as the value of T_G/T_1 is of the order of 5 or greater, the airplane may be treated as a rigid body. Subsequent results will bear out this point further.

It is of interest to note that considering the response factor alone may be misleading, as can be seen in figure 6(b) where the bending-moment factor K_{root} is given; these curves are of primary interest to the designer since they lead to the net incremental bending moment developed, which is the quantity required in the design for gust loads. The loading condition where the load is concentrated near the airplane center line produced the critical bending moment, as would be expected, even though it gave the lowest values of response factor.

Effect of speed and altitude.- The previous results (figs. 4 to 6) are for a constant velocity but for a varying gust-gradient distance. In order to obtain a direct measure of the effect of forward velocity, some calculations were made with all conditions except velocity held constant; in order to obtain also a measure of the effect of altitude, this velocity study was made at two altitudes. Airplane B, with loading condition III (see table 1), was used for this part of the investigation since the results in figure 6(b) show that this loading condition leads to the critical bending moment. This airplane was assumed to fly at various speeds through a sine gust of 10-chord gradient distance at sea level and at an altitude of 25,000 feet (ρ at 25,000 feet was taken as 0.00107 slug/cu ft). Speeds up to 600 mph were considered and, although these speeds may be sufficient in reality to cause flutter, it has been assumed that no flutter troubles or magnification in response due to nearness to flutter will be encountered. The results are shown in figure 7 where the bending-moment factor and the bending-moment response factor are plotted as a function of both the velocity and the period ratio T_G/T_1. (In order to be consistent with previous figures this period ratio is plotted increasing to the right so that velocity increases to the left.) The results at a speed of 255 mph for the sea-level condition are, of course, the same as the results shown in figure 6(a) for H = 10.

For the sea-level condition it may be noted that the extent of the variation of γ_M with T_G/T_1 is much less than is indicated in the previous figures and also that the maximum value of γ_M occurs at a larger value of the period ratio than before. These facts may be ascribed to the aerodynamic damping associated with airplane vertical motion, which damping is known to be proportional to the product ρV. In the previous results the damping is constant since the velocity is fixed at 255 mph. In this case, however, the damping increases with increasing velocity and is always great enough to prevent large dynamic overshoots from occurring, even in the vicinity of $T_G/T_1 \approx 2$ where, on the basis of previous results, large dynamic overshoots would be expected. For the 25,000-foot-altitude condition, the dynamic overshoot is always greater than at sea level - a fact which is also directly related to the aerodynamic damping effects. This damping decreases with altitude because of the decrease in air density, and at 25,000 feet is small enough to allow appreciable dynamic overshoots to occur even at the larger velocities.

It should be noted that, even though the values of γ_M and K_{root} are greater at 25,000 feet than at sea level, the magnitude of the bending moment obtained by equation (1) will be larger at sea level because of the greater air density.

Effect of compressibility and aspect-ratio corrections.- As has been mentioned, the response-factor curves shown in figure 7 and in the previous figures were calculated with the use of the theoretical lift-curve slope and the indicial lift functions for two-dimensional incompressible flow. In order to obtain an indication of how the maximum bending moment is affected by compressibility and aspect-ratio corrections, response calculations for airplane B, loading condition III, were repeated with various approximate schemes for taking into account these effects. A sea-level speed of 550 mph, corresponding to a Mach number of 0.7, was used. Again, as in the previous example, it has been assumed that no flutter troubles or magnifications in response due to nearness to flutter will be encountered.

The procedure used to examine the effects of compressibility and aspect-ratio corrections was to make response calculations for different choices in the slope of the lift curve and the indicial lift functions. Because the wing reference chord is a pertinent quantity in response studies, some calculations for different choices in this quantity have been included for general interest along with these compressibility studies. In all, 14 cases were considered; the indicial functions, the slope of the lift curve, and the reference chord that were used in each of these 14 cases are indicated as part of table 2.

The $1 - \Phi$ and ψ functions used were normalized so as to have an asymptotic value of unity and are shown in figure 8. With the exception of the ψ function for $A = 10$, these functions were taken from the references 1, 4, and 5 as indicated in the table. The ψ function for $A = 10$ was formed by interpolation of the ψ function given in reference 4 and a good approximation to the interpolated results was found to be

$$\psi_{A=10} = 1 - 0.39e^{-0.2S} - 0.61e^{-0.9S}$$

The first value listed for the slope of the lift curve is the theoretical value 2π for incompressible flow. The remaining values represent attempts to take into account aspect-ratio and compressibility effects, separately and jointly; the corrections involved are, respectively, the often-used aspect-ratio correction $\frac{A}{A + 2}$, the Glauert-Prandtl Mach number factor $\frac{1}{\sqrt{1 - M^2}}$, and a factor which approximately takes into account both Mach number and aspect-ratio effects as explained in reference 4, $\frac{A}{2 + A\sqrt{1 - M^2}}$.

The results for the various cases for the condition of flight through a sine gust of 10-chord gradient distance are given on the right-hand side of table 2. By comparing the results for bending moment, a number of points of interest may be noted. First consider the use of different indicial lift functions. With the bending-moment results obtained with the indicial functions for $M = 0$ and $A = \infty$ as a reference, it may be noted that the use of indicial lift functions for $M = 0$ and $A = 10$ leads to a small difference of less than 1 percent in the results. (Compare cases 7, 8, and 10 with cases 1, 2, and 3.) The use of the indicial lift functions for $M = 0.7$ and $A = \infty$ gives a difference that is larger but still less than 6 percent. (Compare cases 11, 12, and 14 with cases 1, 2, and 3.) Next consider the use of different values of the lift-curve slope. (Compare cases 1 to 3, cases 4 to 6, cases 7 to 10, and cases 11 to 14.) In general, the magnitude of the bending moment increases as the value of the lift-curve slope increases and, more specifically, the percentage change in the bending moment is roughly one-fourth to one-half the percentage change in the lift-curve slope. Now consider the use of different reference chords. The use of the mean geometric chord yielded results which are less than 5 percent greater than the results obtained when the midspan chord was used. (Note that the absolute gust-gradient distance for cases 4, 5, and 6 is

different from that for cases 1, 2, and 3 since the results have been obtained on the basis of the same nondimensional gust-gradient distance of $H = 10$ chords.)

Although the trends just noted have been obtained for one airplane, it is felt that they are fairly representative of airplanes having high wing loadings.

Cases 1, 8, and 14 are of special interest since, of all the cases treated, they represent the most nearly self-consistent selections of lift-curve slope and indicial lift functions. Thus, the results of case 1 represent the outcome of applying unsteady-lift theory for ideal two-dimensional incompressible flow; the results of case 8 represent the outcome of applying the unsteady-lift theory for finite-aspect-ratio incompressible flow; and the results of case 14 represent the outcome of applying what might be considered the best available methods for approximately taking into account both aspect-ratio and compressibility effects. Curiously enough, the bending moment for case 14 is almost identical with the bending moment for case 1 where no corrections whatsoever are made; how general this result may be is not known.

EFFECT OF WING FLEXIBILITY ON GUST-LOADS MEASUREMENTS

As the second phase of the calculation studies, the acceleration and bending-moment values that result from discrete gust encounter were determined for each of the airplanes considered herein by the method given in reference 1. These studies were made in order to find out what calculations of this type reveal in regard to the extent that wing bending flexibility might alter gust measurements if such measurements are made with these aircraft. Normally, it has been the practice to measure accelerations at the airplane center line and to deduce from these accelerations the gust intensities. The argument is offered, however, that wing flexibility may cause the accelerations at the center line to be higher than the true (rigid-body component) accelerations, with the consequence that the deduced gusts may be more severe than those actually encountered. This flexibility effect has been investigated experimentally by means of airplanes A and D in flights through clear rough air (see refs. 2 and 3). In these flight investigations accelerometers were mounted at the airplane center line and at the nodal points of the fundamental wing bending mode. For airplane A it was found that the accelerations recorded at the center line due to gusts were, on the average, 20 percent greater than the accelerations at the nodal points. For airplane D this value was about 28 percent.

Calculated Effects

Airplanes A and B.- Airplanes A and B are considered together since, as previously noted, airplane B is a revision of airplane A. Loading condition I, which corresponds roughly to one-half rated pay load and one-half fuel load, was used for both airplanes, and the condition of sine gust encounter was assumed.

A theoretical indication of the extent to which wing flexibility may alter gust measurements if such measurements are made with these airplanes can be obtained by comparing the computed center-line and nodal-point accelerations. (In the method of ref. 1, used to compute these accelerations, the nodal-point and true airplane accelerations are equal.) This comparison is given in figure 9(a) where the ratio γ_a of the maximum incremental center-line acceleration to the maximum incremental nodal acceleration is plotted against the gust-gradient distance and the period ratio T_G/T_1. These results suggest that for both airplanes there would be a substantial difference in the acceleration if measured at the airplane center line than if measured at the nodal point, at least for intermediate gust lengths. Moreover the results indicate that this difference should be essentially the same for both airplanes. For the larger gust lengths of the order of 10 chords or greater or for T_G/T_1 of 5 or greater, very little difference between center-line and nodal-point acceleration would be expected.

Since the bending moments developed are also of interest, especially to the designer, the bending-moment results presented previously in figures 4 and 6 for these airplanes are compared in figures 9(b) and 9(c). It may be seen that the bending-moment response factor γ_M for airplane B is appreciably greater than for airplane A; this fact indicates that airplane B has a characteristically greater dynamic overshoot (at least for this loading condition). This result can be shown to be primarily due to the difference in mass distribution on the wings of the two airplanes. With regard to bending moment, however, there is not a significant difference between the two airplanes. It can be seen from figure 9(c) that for the loading condition considered the bending-moment factor $\left(K_{root}\right)_{max}$ is nearly the same for the two airplanes; hence, the bending moment will also be nearly the same for the two airplanes since the factor $\frac{a}{2}\rho VUM c_0$ in the equation for bending moment (eq. (1)) is common to both airplanes. The stresses developed in airplane B, however, will be less than in airplane A, since airplane B has the greater section modulus at the root station.

Airplane C.- Airplane C has been used extensively in the collection of statistical gust-load data by means of the NACA V-G and VGH recorders. The data thus obtained have been reduced on the basis that the airplane is rigid. In view of the interest in flexibility effects, it was considered desirable to make a gust-response analysis of this airplane as an elastic body to obtain a theoretical measure of the extent to which wing flexibility might have affected the measurements made in flight. The spanwise loading conditions used, the chord and bending stiffness of the wing, and the necessary physical constants are shown in figures 1(c), 2, and 3, and in table 1. The results in terms of acceleration response factor γ_a, bending-moment response factor γ_M, and bending-moment factor $\left(K_{root}\right)_{max}$ are shown in figure 10. It is seen that the response curves for this airplane are significantly different from the response curves for airplanes A and B. Not only are the deviations of the response curves from unity much less, but also these deviations extend over only a narrow range of small gust-gradient distances. The results indicate that, as long as the gust-gradient distance is greater than 5 chords, the treatment of this airplane as a rigid body is justified.

A point of some significance is to be noted when the results for this airplane are viewed in terms of T_G/T_1. Although when viewed in terms of gust-gradient distance airplane C is relatively rigid in comparison with airplanes A and B, it is not so rigid when viewed in terms of T_G/T_1. The response curves peak in the vicinity of $\frac{T_G}{T_1} = 2$ and are not unity in a practical sense until a value of T_G/T_1 of approximately 5 is reached. Thus the rule of thumb cited previously for judging whether or not an airplane is flexible applies even in the case of this more "rigid" airplane.

Airplane D.- This four-engine airplane was chosen partly because it is representative of a size much greater than those previously considered herein and partly because it has a substantial amount of mass distributed over the wing. On the basis of the studies thus far presented, significant values of dynamic overshoot were expected. Figures 1(d), 2, and 3 show the semispan mass, chord, and stiffness distributions; the airplane physical constants are given in table 1. The results of the analysis for the airplane are presented in figure 11 in terms of the bending-moment factor and the response factors for bending moment and acceleration. The results are for a loading condition with most of the disposable load in the wing and with only a small amount of load in the fuselage, even though this loading condition does not lead to the most severe bending moment (see fig. 6). The effect of wing bending flexibility on the response factor for either bending moment or

acceleration is seen to be significant over a wide range of gust-gradient distance. Appreciable differences between center-line and nodal-point accelerations are therefore to be expected with this airplane if it is used for measuring gust intensities. However, a rigid-body analysis would appear to be satisfactory for H greater than approximately 10 chords, or, when judged on a perhaps better basis, for T_G/T_1 greater than 5. It is to be noted that the rule of thumb applies also to this large "flexible" airplane.

Comparison of Calculated Results With Flight Data

As has been mentioned, some acceleration measurements have been made on airplanes A and D while in flight through rough air, and it was considered of interest to see whether the results obtained could be correlated to some extent with theoretical response calculations. Theoretical calculations which could be compared directly with the flight-test data reported in references 2 and 3 could not be made, however, because the gust intensities encountered in the test flights were not evaluated; only accelerations and wing strains were established. An indirect comparison was therefore made as follows.

Center-line and nodal-point accelerations due to encountering discrete triangular gusts of various gradient distances and various peak gust velocities were computed for both airplanes A and D; the gusts were assumed to be uniform spanwise. The calculations were carried out for each airplane with the indicial-lift functions for $A = 10$, the mid-span reference chord, and a lift-curve slope of $2\pi \frac{A}{A + 2}$. The loading conditions shown in table 1 were used since these loading conditions correspond closely to the conditions used in the flight tests reported in references 2 and 3. The results are shown as the radial lines from the origin in figure 12, where the maximum incremental acceleration developed at the airplane center line is plotted against the maximum incremental acceleration at the nodal point of the fundamental mode, the latter being a measure of the maximum average vertical acceleration of the airplane. The radial lines are for different gust-gradient distances and, in order to show the influence of gust intensity, the results for three gust velocities, $U = 15$, 30, and 45 fps, are shown as points on these lines.

The shaded bands shown in this figure represent the portions of the theoretical calculations that apply when a measure of empiricism regarding realistic gust sizes is introduced. These bands were established by considering the gust data shown in figure 13, which is a reproduction in part of figure 11 in reference 6. The data in this figure represent information that was gathered during flight operation

in thunderstorms and were deduced on the basis that the gusts encountered were triangular in shape and uniform in the spanwise direction. An index of the limits on gust sizes that might be encountered in practice can be established by drawing the envelope curve for these data. The envelope curve assumed herein is the solid curve shown in figure 13. Consideration of all the gusts that are defined by this envelope curve leads to the upper limit of the bands shown in figure 12. (Because the assumptions of uniform spanwise intensity and discrete gust encounter are less plausible for the smaller gusts, the upper limit has been left blank in the vicinity of the origin.) The lower limit is simply the curve which defines rigid-body behavior of the airplane. Thus, in short, if calculations were made for all the gusts shown in figure 13, all the acceleration values obtained would fall within the bands shown in figure 12. Since the gusts shown in figure 13 were encountered during severe operating conditions, it is logical to expect that all gusts that are encountered in normal flight would give theoretical acceleration values which would also fall within these bands.

In figure 14, a comparison is made of the bands established in this manner with the flight data reported in references 2 and 3. Figure 14(a) applies to airplane A and contains the flight data of reference 2 for run A; figure 14(b) applies to airplane D and contains the flight data of reference 3 for the wing-heavy, 250-mph flight condition. Unfortunately most of the flight data are for small gusts (low accelerations), out of the range where it is reasonable to expect this theoretical approach to apply. It appears, however, that the envelope curve of the flight data can be predicted with fair accuracy, as evidenced by the rather nice way the flight data merges into the calculated bands.

CONCLUDING REMARKS

In this report, results of calculated case-history studies made to investigate the role that wing bending flexibility plays in the structural response of an airplane penetrating a gust have been presented for three twin-engine transports and one four-engine bomber. The method of analysis used considers the airplane to have two degrees of freedom, rigid-body vertical motion and fundamental wing bending.

The calculations were made for the condition of a single gust encounter and the factors investigated included gust-gradient distance, gust shape, disposition of movable load, forward velocity, altitude, and compressibility and aspect-ratio corrections. The means for indicating flexibility effects are to compare accelerations at the airplane center line with the rigid-body (nodal point) component of acceleration and to compare wing bending moments for the flexible airplane with the moments obtained for the airplane considered rigid. One significant result

obtained from these comparisons is a rule of thumb which states (on the basis of sine gust encounter) that as long as the period ratio, the time to penetrate the gust to the point of maximum gust velocity divided by one-fourth the natural period of the fundamental wing bending mode, is of the order of 5 or greater, the airplane may be treated as a rigid body. These comparisons also indicate that three of the airplanes have rather appreciable elastic-body dynamic-overshoot effects but one does not.

Some of the other results indicated are: The use of indicial lift functions for finite-aspect-ratio wings and for two-dimensional compressible flow gave results which were less than 1 percent and 6 percent different, respectively, from the results that were obtained when the indicial functions for two-dimensional incompressible flow were used; the use of different values of the lift-curve slope gave a percentage change in the root bending moment which was roughly one-fourth to one-half the percentage change in lift-curve slope.

Also, a limited correlation of theoretical results with rough-air flight data showing the relation between center-line and nodal-point accelerations indicates that an envelope for these data can be predicted with fair accuracy.

Langley Aeronautical Laboratory,
National Advisory Committee for Aeronautics,
Langley Field, Va., November 20, 1952.

REFERENCES

1. Houbolt, John C., and Kordes, Eldon E.: Gust-Response Analysis of an Airplane Including Wing Bending Flexibility. NACA TN 2763, 1952.

2. Shufflebarger, C. C., and Mickleboro, Harry C.: Flight Investigation of the Effect of Transient Wing Response on Measured Accelerations of a Modern Transport Airplane in Rough Air. NACA TN 2150, 1950.

3. Mickleboro, Harry C., Fahrer, Richard B., and Shufflebarger, C. C.: Flight Investigation of Transient Wing Response on a Four-Engine Bomber Airplane in Rough Air With Respect to Center-of-Gravity Accelerations. NACA TN 2780, 1952.

4. Houbolt, John C.: A Recurrence Matrix Solution for the Dynamic Response of Aircraft in Gusts. NACA Rep. 1010, 1951. (Supersedes NACA TN 2060.)

5. Mazelsky, Bernard: Numerical Determination of Indicial Lift of a Two-Dimensional Sinking Airfoil at Subsonic Mach Numbers From Oscillatory Lift Coefficients With Calculations for Mach Number 0.7. NACA TN 2562, 1951.

6. Donely, Philip: Summary of Information Relating to Gust Loads on Airplanes. NACA Rep. 997, 1950. (Supersedes NACA TN 1976.)

TABLE 1.- AIRPLANE PHYSICAL CONSTANTS, LOADING, AND BASIC PARAMETERS

	Airplane A	Airplane B			Airplane C	Airplane D
[a]Loading condition	I	I	II	III	IV	V
W, lb	33,470	34,930	34,960	34,900	24,140	108,480
S, sq ft	870	870	870	870	987	1,739
b, in.	560	560	560	560	570	850
a	6.28	6.28	6.28	6.28	6.28	6.28
c_o, in.	164	164	164	164	170	205
A	10	10	10	10	9	11.6
V, mph	255	255	255	255	210	250
ρ, slugs/cu ft	0.00238	0.00238	0.00238	0.00238	0.00238	0.00238
ω_1, radians/sec	21.4	20.8	14.9	24.0	28.0	15.4
μ_0	46.8	49.0	49.0	48.8	28.8	60.9
μ_1	0.748	1.117	2.155	0.787	0.262	1.130
λ	0.392	0.378	0.273	0.439	0.639	0.359
r_1	0.225	0.206	0.167	0.234	0.192	0.189
r_2	0.143	0.140	0.133	0.144	0.096	0.129
r_3	0.457	0.444	0.412	0.462	0.367	0.417
η_0	15.94	20.30	29.10	13.30	6.77	31.32
η_1	2.56	3.64	6.16	2.53	0.954	3.73
M_{c_0}, ft^3	6,680	6,680	6,680	6,680	7,320	22,750

[a]I Approximately one-half load and one-half fuel.
II Approximately zero load and full fuel.
III Approximately full load and zero fuel.
IV Full load and one-half fuel.
V Full crew, zero load, and wing tanks full.

TABLE 2.- RESULTS OF COMPRESSIBILITY AND ASPECT-RATIO STUDIES OF AIRPLANE B

[Loading condition III; V = 550 mph; H = 10 chords; sine gust]

Case	$1 - \phi$ and ψ functions for -			Lift-curve slope, a (1)				Reference chord, c_0		$\left(K_{root}\right)_{max}$ for flexible airplane	$\left(K_{root}\right)_{max}$ for rigid airplane	γ_M	$\frac{\left(M_{root}\right)_{max}}{U}$ for flexible airplane, lb-sec
	M = 0, A = ∞ (refs. 1 and 4)	M = 0, A = 10 (ref. 4)	M = 0.7, A = ∞ (ref. 5)	2π = 6.28	$\frac{2\pi A}{A+2}$ = 5.83	$\frac{2\pi}{\sqrt{1-M^2}}$ = 8.97	$\frac{2\pi A}{2 + A\sqrt{1-M^2}}$ = 6.98 (ref. 4)	Midspan chord, 164 in.	Mean geometric chord, 112 in.				
1	✓			✓				✓		0.441	0.459	0.962	17,770
2	✓				✓			✓		.491	.486	1.012	16,480
3	✓						✓	✓		.416	.446	.913	18,640
4	✓			✓					✓	.454	.511	.888	18,300
5	✓				✓				✓	.511	.637	.952	17,150
6	✓						✓		✓	.426	.499	.854	19,080
7		✓		✓				✓		.440	.476	.924	17,730
8		✓			✓			✓		.493	.502	.982	16,550
9		✓				✓		✓		.340	.415	.819	19,570
10		✓					✓	✓		.413	.461	.896	18,500
11			✓	✓				✓		.420	.423	.993	16,930
12			✓		✓			✓		.464	.444	1.045	15,580
13			✓			✓		✓		.334	.376	.888	19,220
14			✓				✓	✓		.397	.411	.966	17,790

[1]Evaluated for A = 10 and M = 0.7.

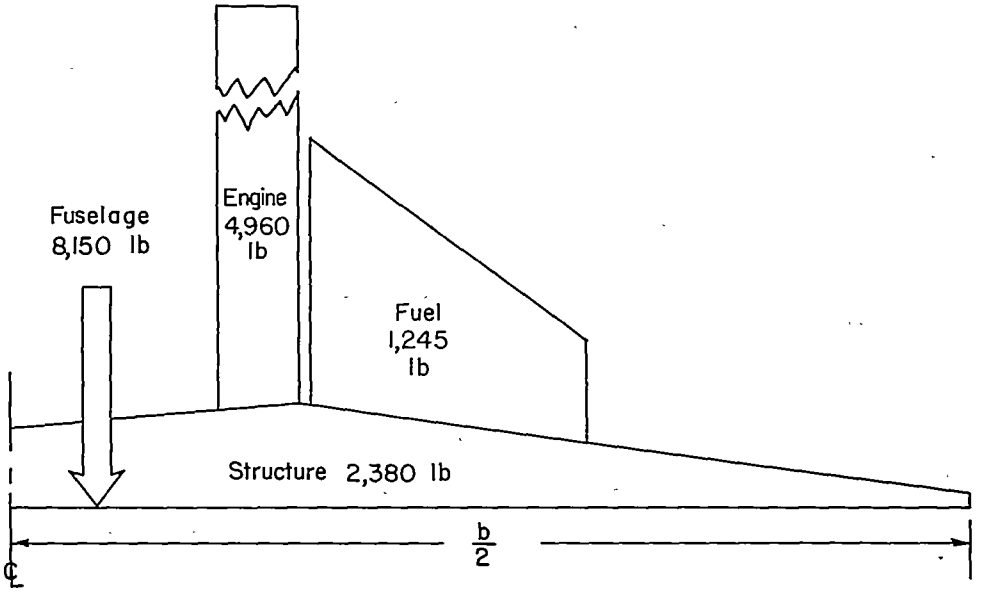

(a) Airplane A.

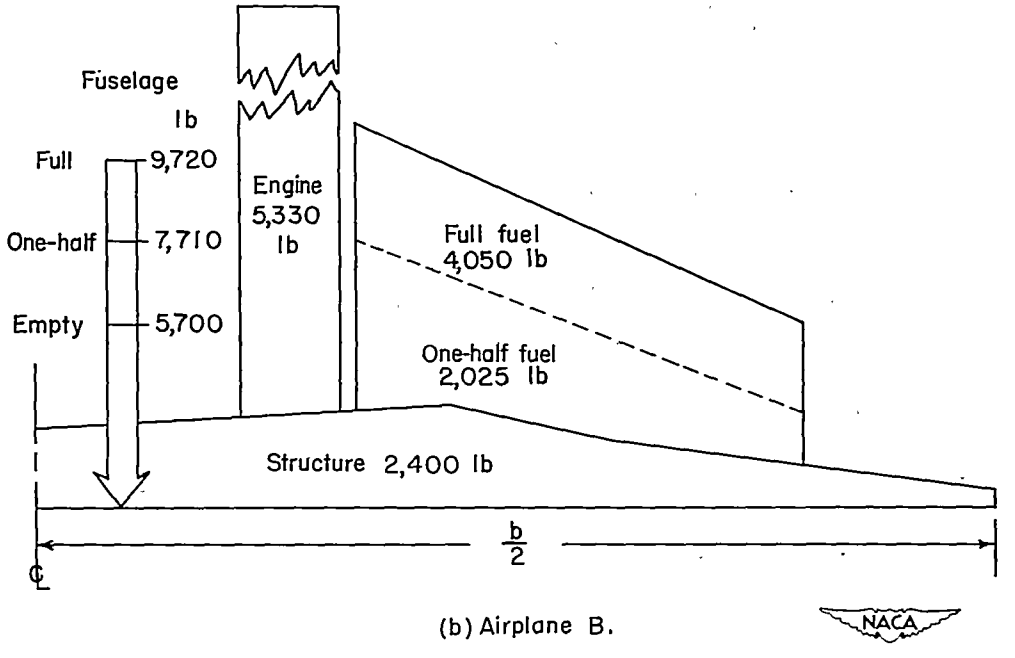

(b) Airplane B.

Figure 1.- Distribution of mass along wing semispan.

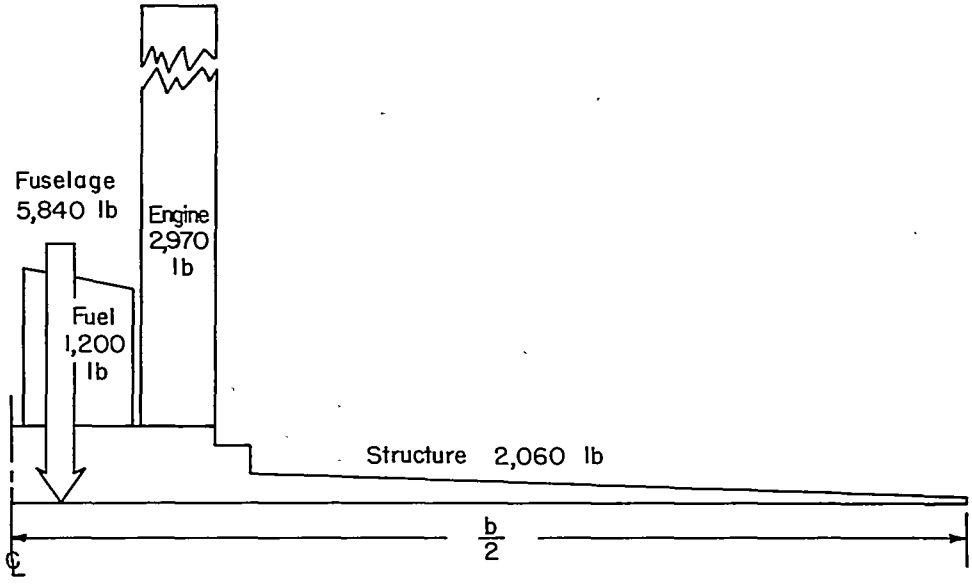

(c) Airplane C.

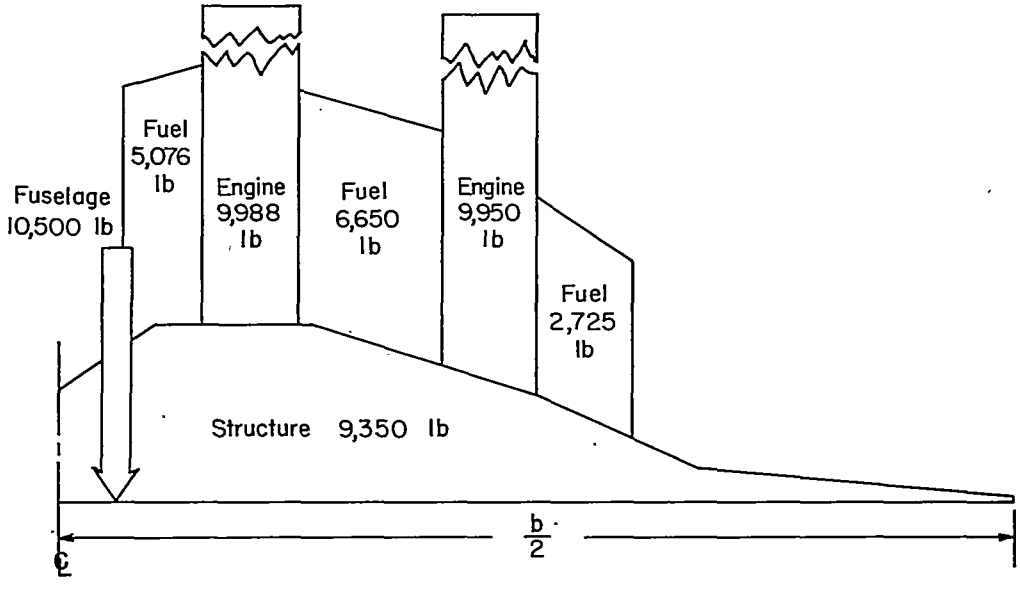

(d) Airplane D.

Figure 1.– Concluded.

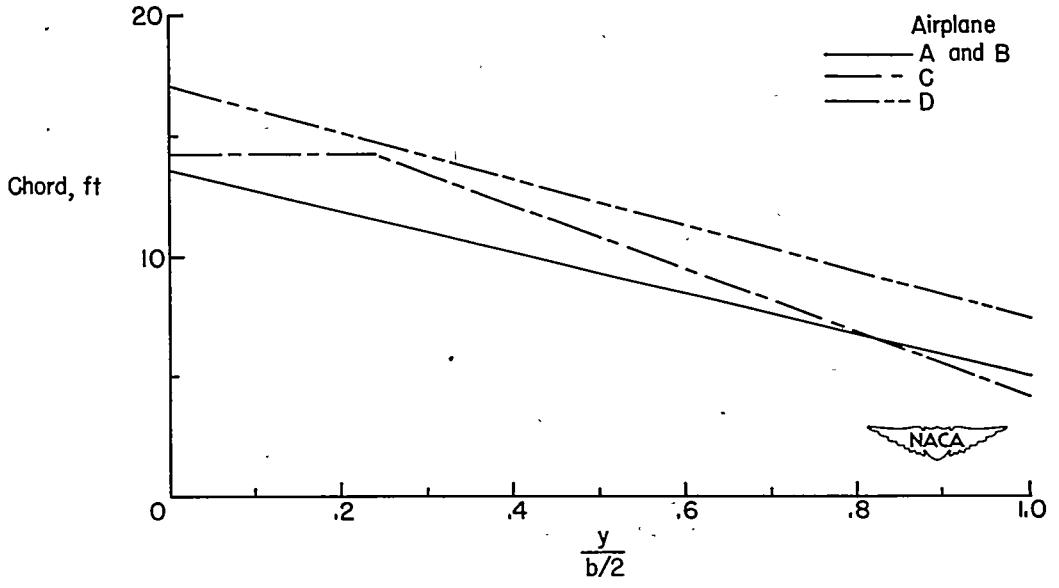

Figure 2.- Variation of wing chord along semispan.

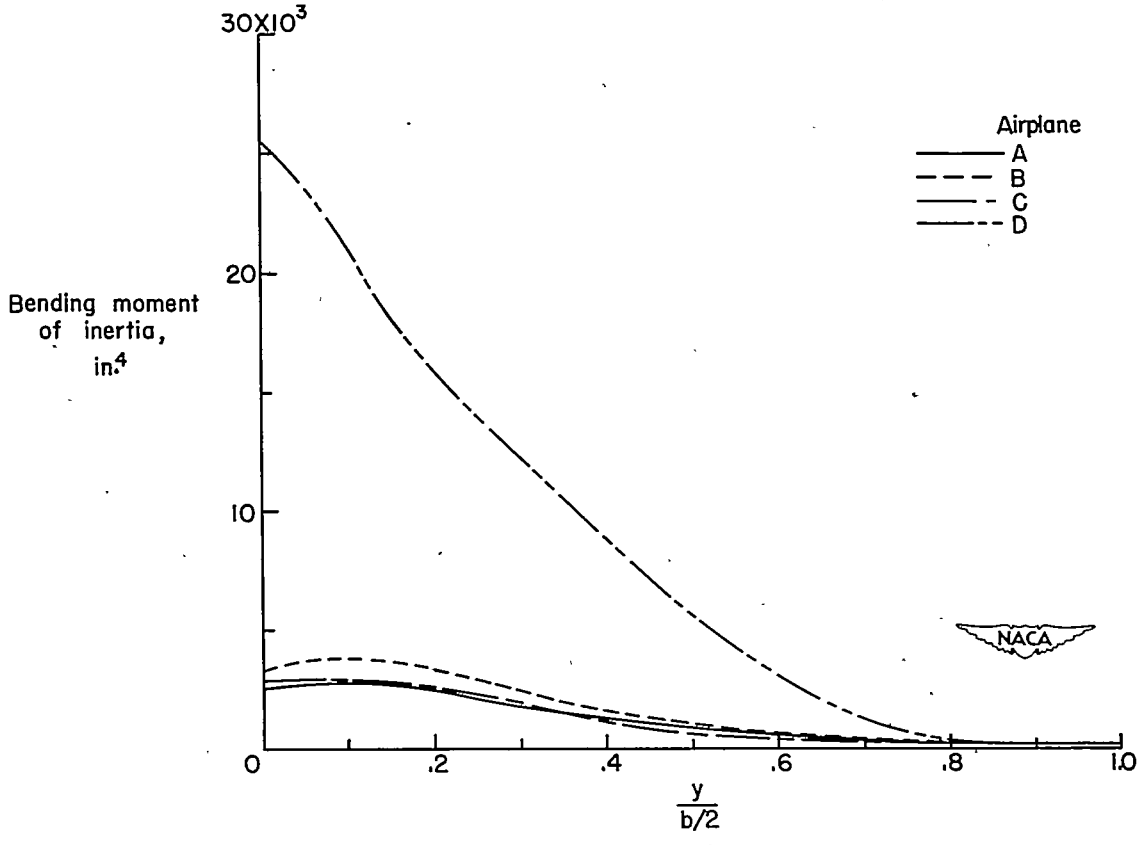

Figure 3.- Variation of bending moment of inertia along semispan.

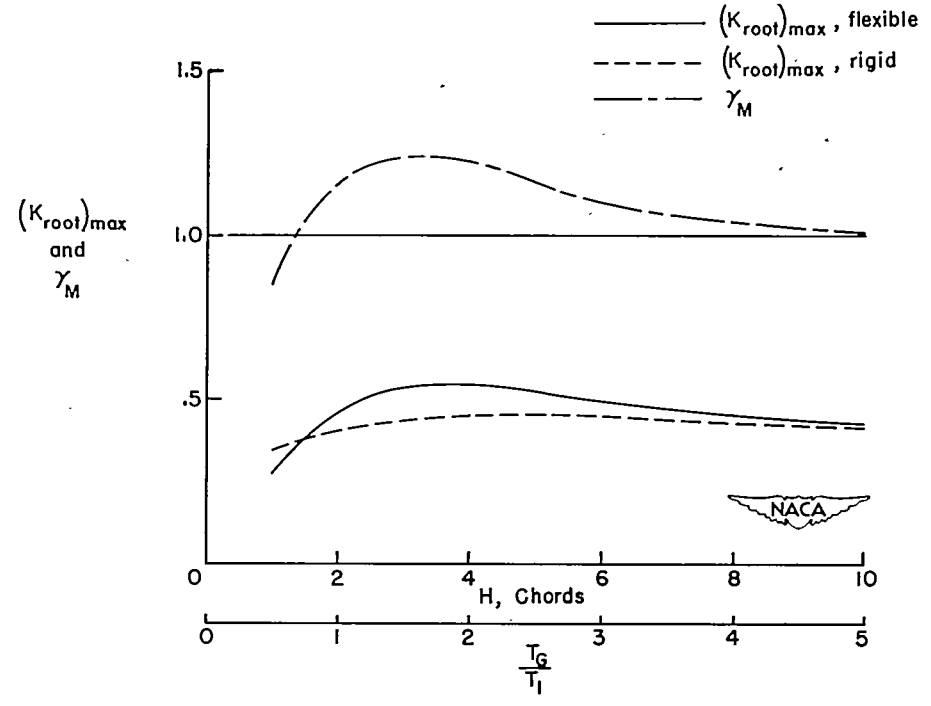

Figure 4.- Effect of gust-gradient distance on $(K_{root})_{max}$ and γ_M for airplane A. Loading condition I; V=255 mph. Sine gusts.

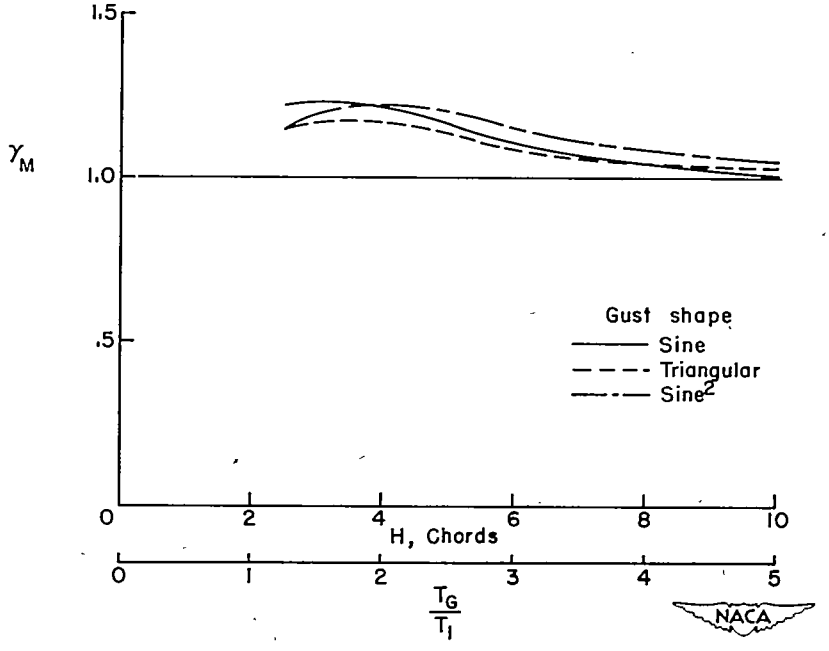

Figure 5.- Effect of gust shape on γ_M as obtained for airplane A. Loading condition I; V=255 mph.

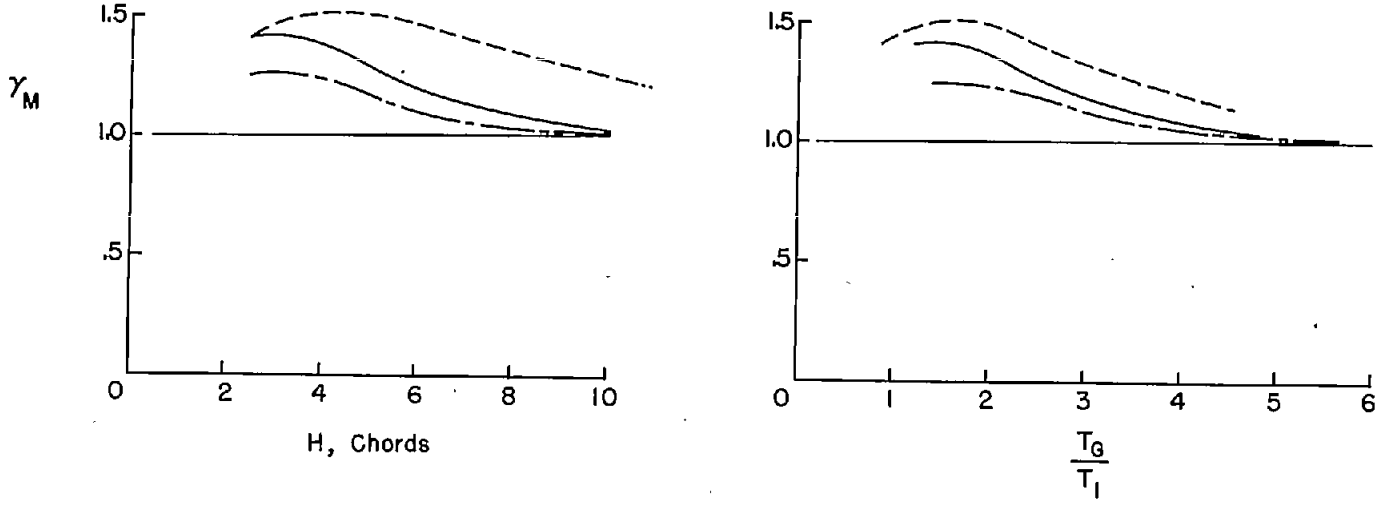

(a) Bending-moment response factor.

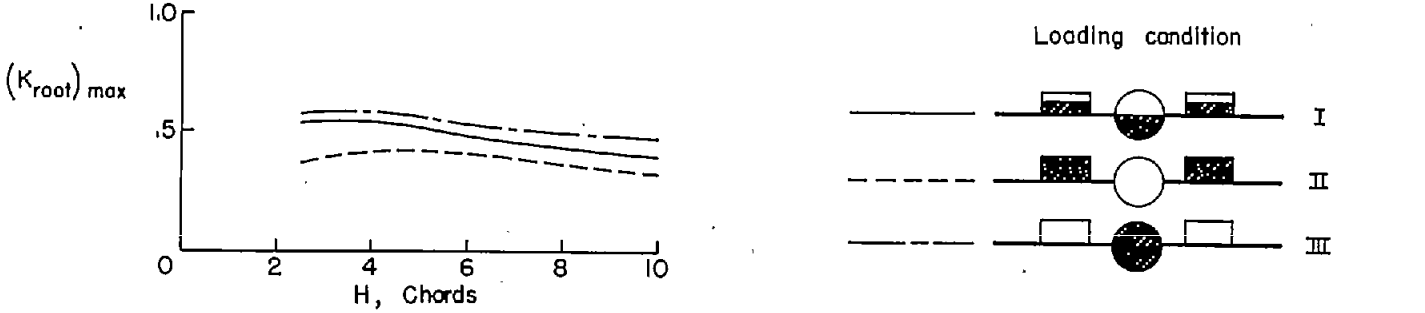

(b) Bending-moment factor.

Figure 6.- Effect of distribution of movable load on $(K_{root})_{max}$ and γ_M as obtained for airplane B. V=255 mph. Sine gusts.

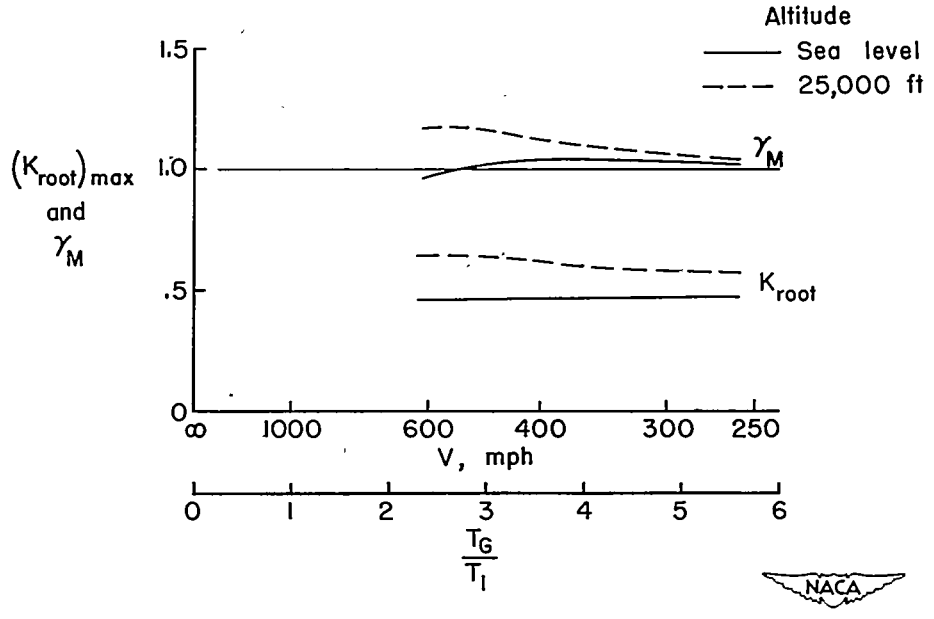

Figure 7.- Effect of speed and altitude on $(K_{root})_{max}$ and γ_M as obtained for airplane B. Loading condition III. Sine gust; H=10 chords.

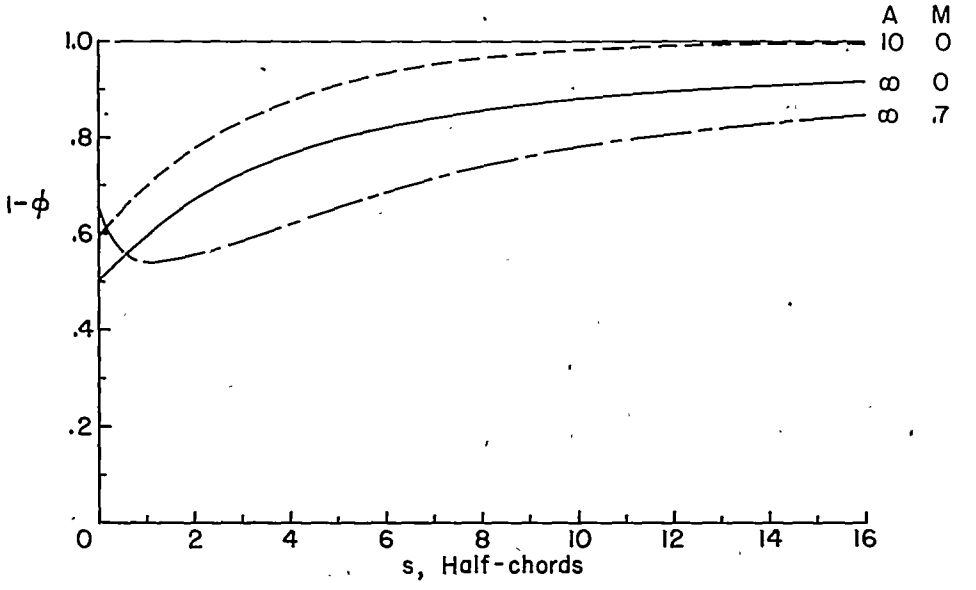

(a) $1-\phi$ function.

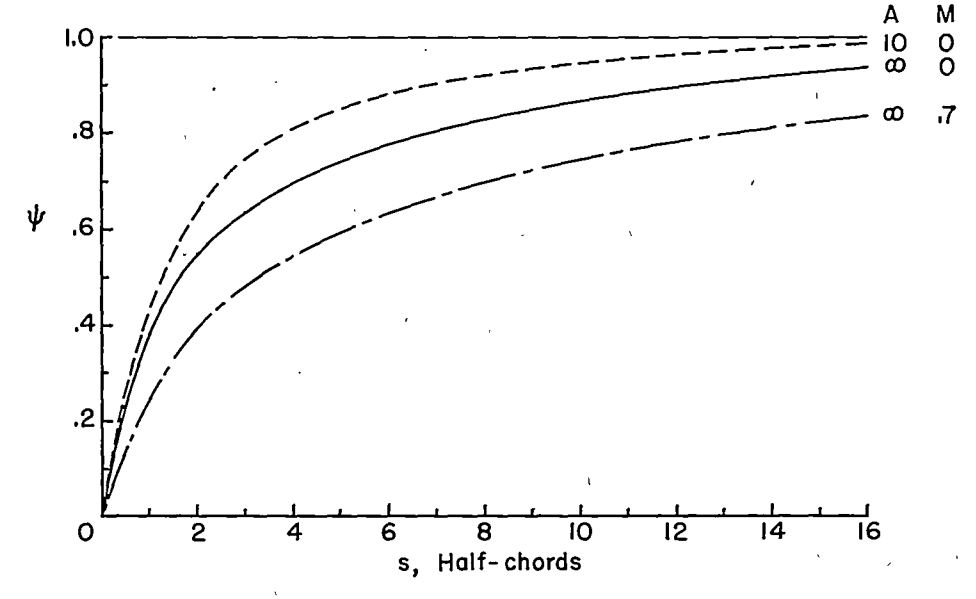

(b) ψ function.

Figure 8.- Unsteady-lift functions.

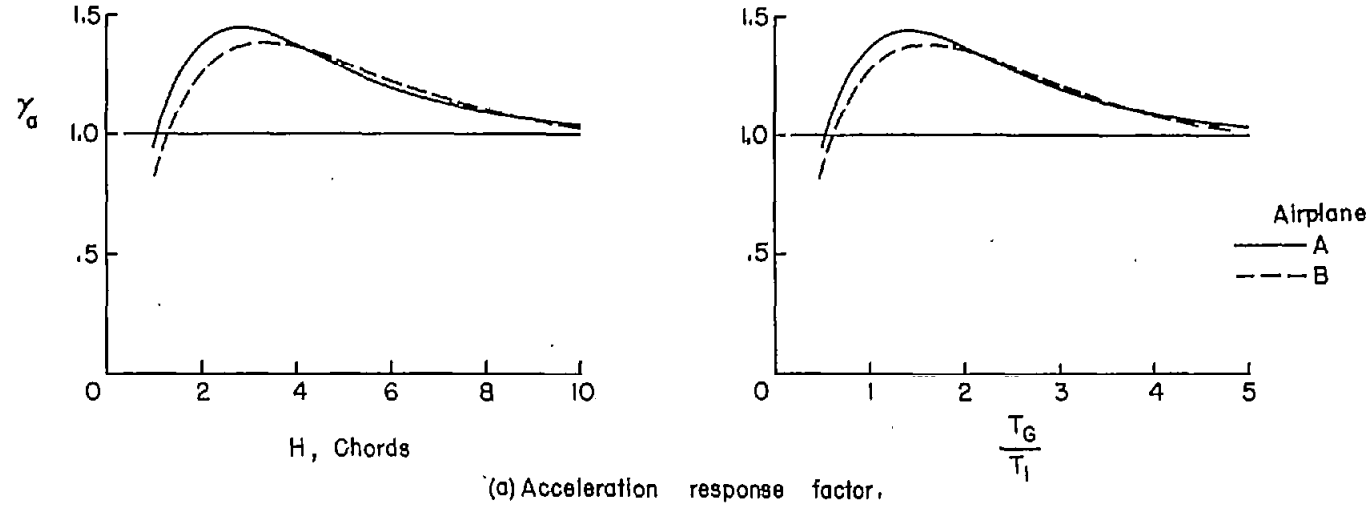

(a) Acceleration response factor.

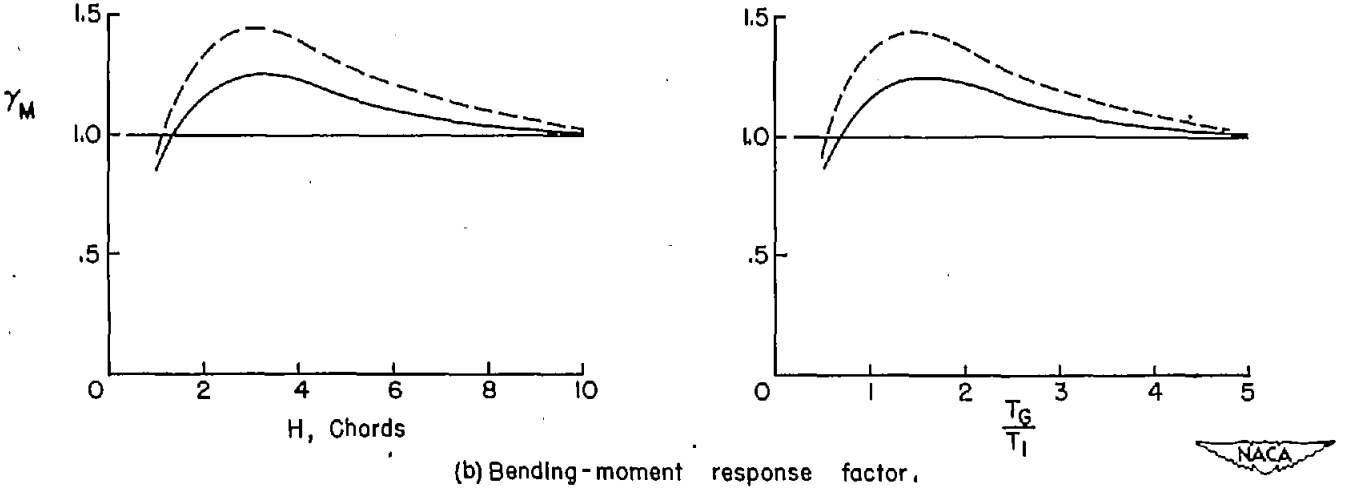

(b) Bending-moment response factor.

Figure 9.- Variation of $(K_{root})_{max}$, γ_M, and γ_a with gust-gradient distance for airplanes A and B. Loading condition I; V=255 mph. Sine gusts.

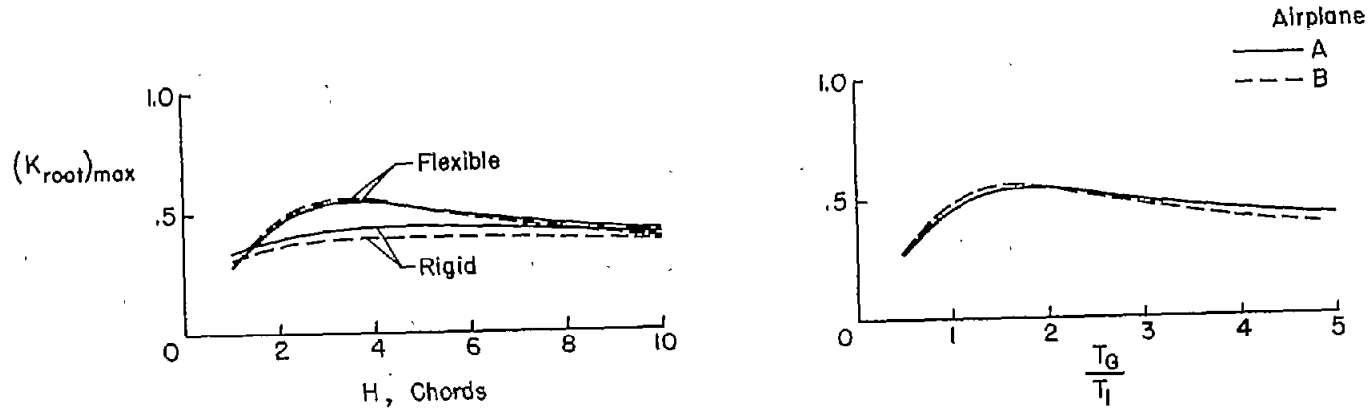

(c) Bending-moment factor.

Figure 9.- Concluded.

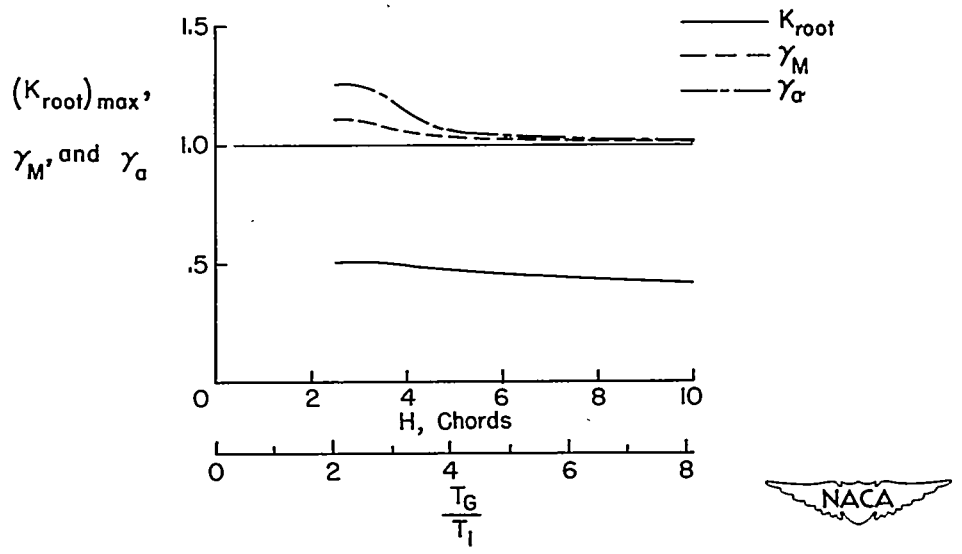

Figure 10.- Variation of $(K_{root})_{max}$, γ_M, and γ_a with gust-gradient distance for airplane C. Loading condition IV; V=210 mph. Sine gusts.

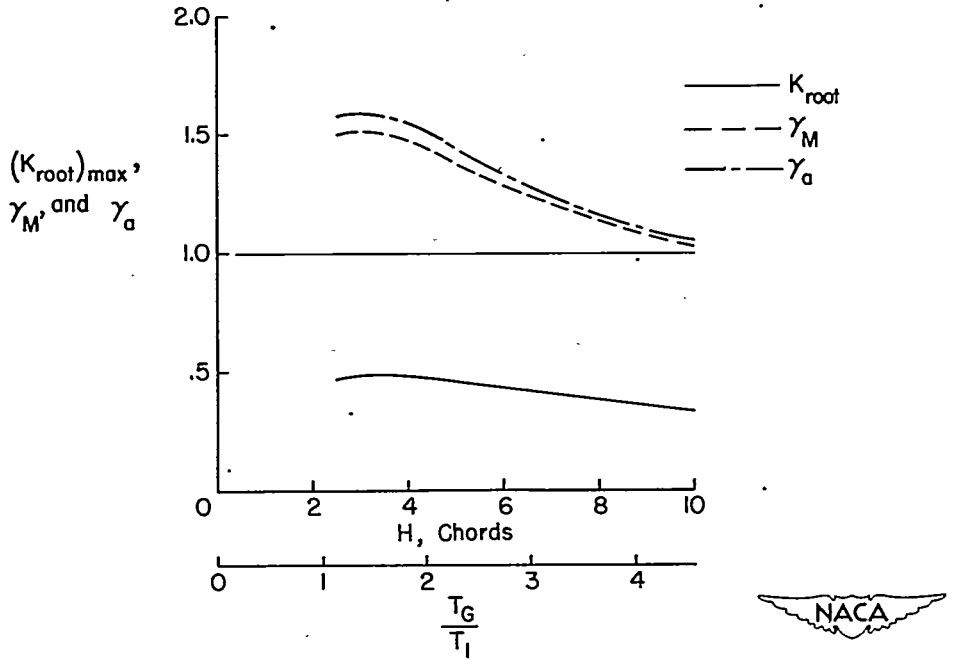

Figure 11.- Variation of $(K_{root})_{max}$, γ_M, and γ_a with gust-gradient distance for airplane D. Loading condition V; V=250 mph. Sine gusts.

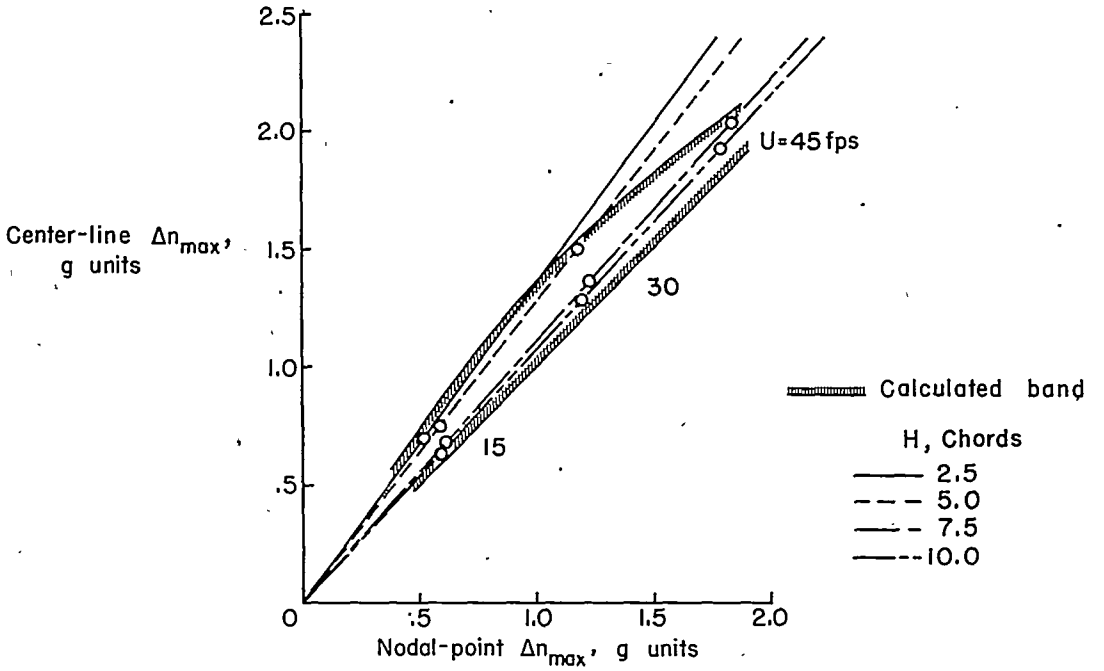

(a) Airplane A with loading condition I.

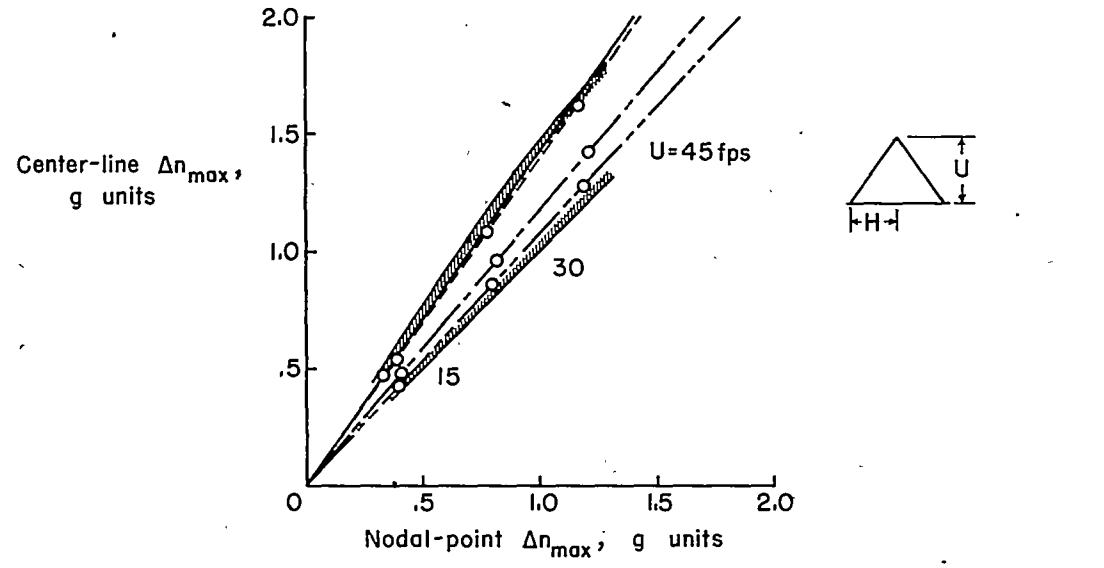

(b) Airplane D with loading condition V.

Figure 12.- Comparison of calculated center-line accelerations with calculated nodal-point accelerations for airplanes A and D.

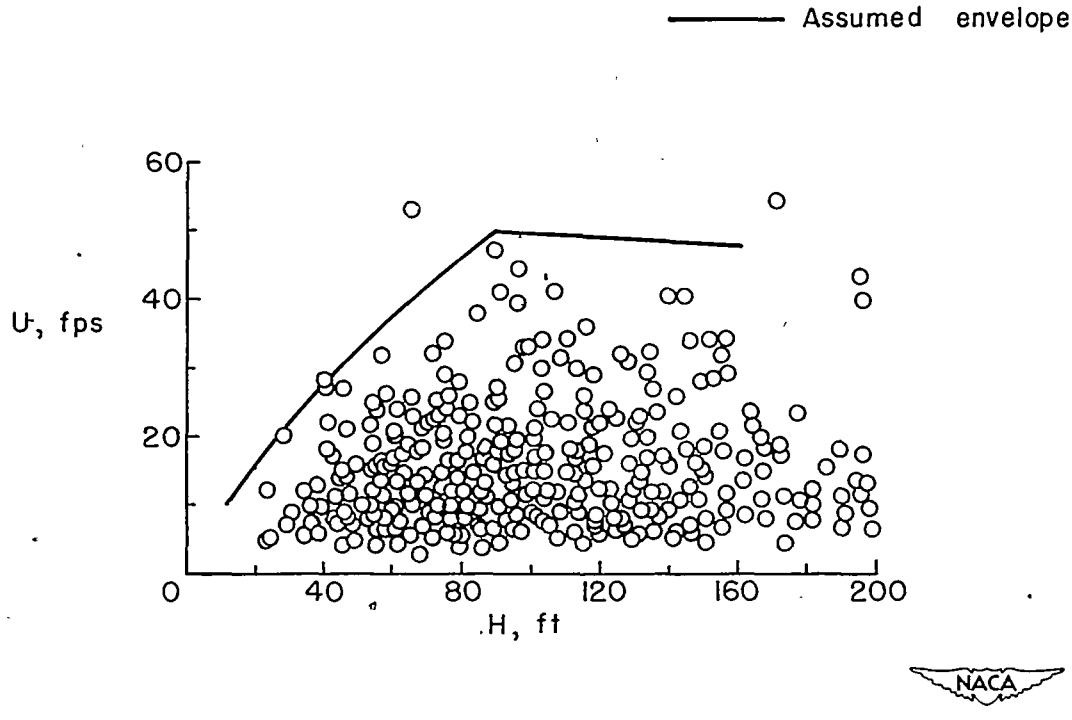

Figure 13.- Data obtained during flight in thunderstorms. (See ref. 6.)

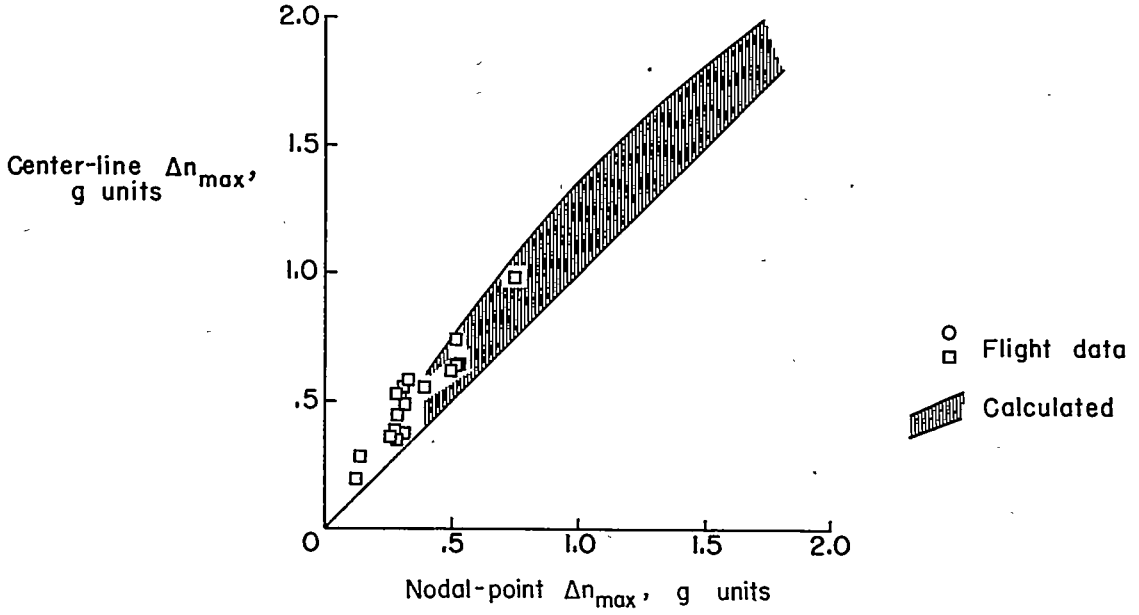

(a) Airplane A. (Run A, ref. 2.)

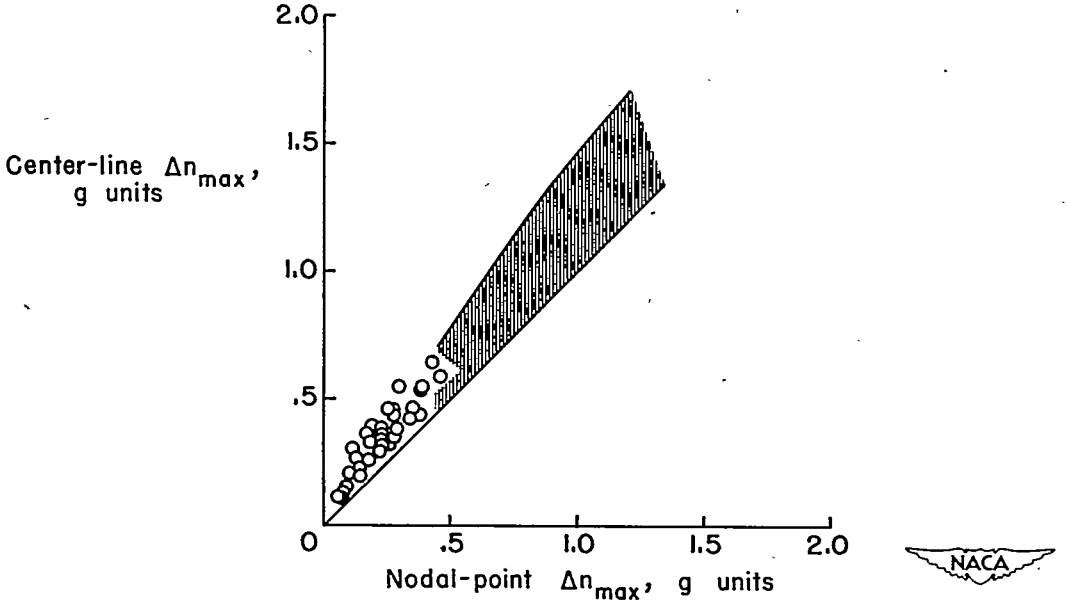

(b) Airplane D. (Wing-heavy, 250-mph flight condition, ref. 3.)

Figure 14.- Comparison of acceleration values established in rough-air flight with calculated values.

NACA-Langley - 2-25-53 - 1000